



Cite this: *RSC Appl. Polym.*, 2025, **3**, 1531

## Fabrication of biodegradable and active pectin-based films with enhanced properties by the incorporation of natural eutectic solvents

Marianela Zoratti,<sup>a,b</sup> Pablo A. Mercadal,<sup>\*a,b,c</sup> Paola A. Gimenez,<sup>a,b</sup> Matias L. Picchio  <sup>d,e</sup> and Agustín González<sup>\*a,b</sup>

Achieving biodegradable and functional food packaging with enhanced mechanical resistance, barrier efficiency, and bioactive properties remains a challenge. This study investigates the incorporation of natural eutectic solvents (NAES) as a strategy to improve the performance of pectin-based films. These NAES, composed of choline chloride (ChCl) and tannic acid (TA) or citric acid (CA), were added at concentrations of 67 and 80 wt% to develop materials suitable for food packaging applications. The films were fabricated via a casting method, and their structural, physicochemical, and functional characteristics were thoroughly analyzed. Results revealed that NAES played a key role in reinforcing the mechanical properties of the films, increasing their tensile strength from  $\approx 0.75$  MPa in the control samples to  $\approx 2.2$  MPa. Additionally, the presence of NAES significantly improved the films' capacity to block UV radiation, particularly in the 200–350 nm range, which is crucial for preserving light-sensitive food products like polyunsaturated oils. Environmental sustainability was also confirmed through biodegradation assays, where the films exhibited an 80% weight loss after 20 days in soil. Furthermore, antimicrobial properties conferred by NAES effectively inhibited the growth of *E. coli* and *S. aureus*, with inhibition zones surpassing 15 mm. When applied to food preservation, the films provided remarkable oxidative protection to chia oil, reducing hydroperoxide levels from approximately 57 to 7.5 meqO<sub>2</sub> kg<sup>-1</sup> oil, while extending the oxidation induction period from 0.25 to  $\approx 4.6$  hours over 25 days of storage in oxidative accelerated conditions. These findings underscore the potential of NAES as active additives that enhance the properties of bio-polymer-based films while imparting bioactive functionality, paving the way for sustainable and efficient food packaging solutions.

Received 6th April 2025,  
Accepted 1st September 2025

DOI: 10.1039/d5lp00099h  
[rsc.li/rscapplpolym](http://rsc.li/rscapplpolym)

## Introduction

In recent years, there has been a significant push toward sustainability in the industry, with a particular focus on the food packaging sector.<sup>1</sup> In this sense, the emphasis is placed on utilizing proteins or polysaccharides from renewable resources such as chitosan, gelatin, soy protein, casein, zein, and pectin.<sup>2,3</sup> Among these, pectin (PEC) which is a polysaccharide,

is particularly attractive for being sourced from fruit waste like apple pomace and citrus peels, presenting an eco-friendly option with excellent biodegradability and minimal environmental impact. As a food-grade material, PEC meets the growing consumer demand for safe and sustainable packaging solutions.<sup>4</sup> However, the broader implementation of PEC-based films is constrained by their insufficient mechanical properties and inadequate barrier capabilities against oxygen, moisture, and UV/visible light. The industry also seeks active packaging solutions that can interact with food to extend its shelf life through antioxidant, antifungal, and antibacterial activities.<sup>5</sup>

To mitigate these shortcomings, prevalent strategies include blending multiple biopolymers to create composite films, incorporating nanoparticles, and adding functional additives that promote crosslinking or provide plasticizing effects. In addition, several efforts have been made to facilitate the active properties of films such as antioxidant or antibacterial activity.<sup>6</sup> For example, curcumin and silver nanoparticles in a PEC/gelatin blend demonstrate good mechanical and *in vitro*

<sup>a</sup>Universidad Nacional de Córdoba, Facultad de Ciencias Químicas, Departamento de Química Orgánica, Córdoba (5000), Argentina.

E-mail: agustingonzalez@unc.edu.ar

<sup>b</sup>Instituto de Investigación y Desarrollo en Ingeniería de Procesos y Química Aplicada (IPQA-CONICET), Córdoba (5000), Argentina

<sup>c</sup>Universidad Nacional de Córdoba, Facultad de Ciencias Agropecuarias, Departamento de Recursos Naturales, Córdoba (5000), Argentina

<sup>d</sup>POLYMAT, Department of Mining-Metallurgy Engineering and Materials Science, School of Engineering, University of the Basque Country (UPV/EHU), Plaza Torres Quevedo 1, 48013 Bilbao, Spain. E-mail: matiasluis.picchio@ehu.eus

<sup>e</sup>IKERBASQUE, Basque Foundation for Science, Plaza Euskadi 5, Bilbao, 48009 Spain



antimicrobial and antioxidant activities but lack real food application examples and antifungal activity.<sup>7</sup> Similarly, polyphenol nanoparticles as fillers in PEC-based films enhance antioxidant and antibacterial properties in strawberries, yet they fall short in antifungal performance.<sup>8</sup> Additionally, cross-linking PEC-based films with vanillin and  $\text{Fe}^{3+}$  improves mechanical performance and gas barrier properties, suitable for preserving cherry tomatoes, but lacks comprehensive microbial protection.<sup>9</sup> Furthermore, the production of these films involves several steps, which complicates scaling to industrial levels due to their complexity.<sup>10</sup>

A more recent approach is the use of natural eutectic solvents (NAES), which are environmentally friendly liquids composed of at least one hydrogen bond donor (HBD) and acceptor (HBA). With low vapor pressure and customizable chemical properties, NAES can be formulated from a diverse array of active compounds.<sup>11,12</sup> The utilization of this NAES in biopolymeric matrices offers considerable benefits, including its stabilization,<sup>13</sup> crosslinking or plasticizing effects, the possibility to obtain high concentrations of compounds with antioxidant, antifungal, and antimicrobial activities, as well as biodegradability and cost-effectiveness.<sup>14,15</sup> Additionally, NAES can be easily incorporated into filmogenic matrices without multiple complex steps, simplifying industrial scaling.<sup>16</sup> Previous attempts to incorporate binary NAES, such as tannic acid (TA)-based NAES to develop soy protein films, have demonstrated improvements in mechanical performance, high antioxidant properties, and antimicrobial activity against specific bacteria strains.<sup>15</sup> In turn, the incorporation of citric acid (CA)-based NAES to develop films results in excellent antimicrobial activity but poor antioxidant properties.<sup>15,17</sup>

Based on these preliminary results, it is promising to use TA and CA-based NAES in formulating PEC-based films. Unlike soy protein matrices derived directly from agricultural products, PEC can be sourced from fruit waste, making it a more sustainable option for eco-friendly packaging solutions. In addition, PEC has demonstrated inherent antimicrobial and antioxidant properties,<sup>18,19</sup> which soy protein does not have. These intrinsic qualities of PEC could be enhanced by incorporating these active NAES, improving not only functionality but also the mechanical and barrier properties of the biopolymer films. In turn, the limitations associated with the modest antioxidant capacity of CA and the inadequate antibacterial activity against Gram-negative bacterial strains of TA could potentially be overcome.

Building on this premise, in this work, we have employed a high concentration of binary NAES based on choline chloride (ChCl) combined with TA or CA to develop biodegradable, environmentally friendly PEC-based films. We conducted an integrated analysis to evaluate their structural characteristics, mechanical properties, water resistance, UV-light barrier, vapor barrier properties, and biodegradability, alongside *in vitro* antioxidant and antibacterial activities. Finally, using chia oil as a real food sample, we assessed their antioxidant effectiveness to demonstrate the practical applicability of these films in the food packaging field.

## Experimental section

### Materials

All used reagents were of analytical grade: pectin (PEC) (Pura Química, Córdoba, Argentina); anhydrous glycerol (Cicarelli, 99.5%); tannic acid (Bio Pack, ≥99%); choline chloride (Sigma Aldrich, ≥99%); anhydrous citric acid (Bio Pack, ≥99.5%); 2,2-diphenyl-1-picrylhydrazyl, Trolox (Sigma Aldrich); absolute ethyl alcohol (Cicarelli, 99.5%),  $\text{CaCl}_2$  (Cicarelli, ≥99.5%); distilled water was used throughout the work.

### Preparation of NAES

The NAES were prepared using the heating method where the HBD and HBA were mixed and heated at 90 °C under constant stirring until a homogeneous liquid was obtained. The as-prepared NAES were: choline chloride/citric acid (ChClCA) in a molar ratio of 2 : 1, and choline chloride/tannic acid (ChClTA) in a molar ratio of 20 : 1, respectively.<sup>15</sup>

### Synthesis of films

The PEC-based films were fabricated using a casting technique. Initially, 0.90 g of PEC was dissolved in 45 mL of distilled water and stirred continuously at 70 °C for 30 minutes. After this, the solutions were blended with the NAES at concentrations of 200 and 400 wt% relative to the PEC mass. The mixture was done at 70 °C and 200 rpm for 30 minutes and then degassed under vacuum for 15 minutes to remove air bubbles. Subsequently, these mixtures were poured into silicone molds measuring 44 cm<sup>2</sup> and dried at 60 °C for 24 hours. The films were de-molded and stored at room temperature. For control samples, glycerol was used in place of NAES at the same concentrations.

### Determination of film thickness

A hand-held micrometer (model ESP1-0001PLA, manufactured in Schwyz, Switzerland) was employed to measure the thickness of each film, averaging ten readings per sample. The calculated average thickness was then used to assess the mechanical properties and opacity of the films.

### Transmittance and opacity of films

A UV-vis spectrophotometer (Shimadzu 1800) was used to record the transmittance spectra of the films with air as the background. The spectra were recorded at room temperature in 1 nm steps, ranging from 200 to 800 nm.

Opacity was assessed by determining the area under the absorption curve within 400 and 800 nm. Rectangular samples of 3.5 × 1.0 cm were used, and the area values were normalized by the film thickness.

### FTIR analysis

The PEC-based films were characterized by Fourier Transform Infrared Spectroscopy using a Nicolet 5-SXC spectrometer (Thermo Fisher Scientific, Waltham, USA) by Attenuated Total Reflectance (ATR-FTIR). A 45° angle of incidence ZnSe crystal was used. To ensure the homogeneity of each sample, different



areas of the films were analyzed. The spectra of NAES were recorded in reflection mode by placing the sample on a gold mirror. An average of 32 scans was collected with a resolution of  $4\text{ cm}^{-1}$ .

### Morphologic characterization of films

The surface morphology of the films was investigated using scanning electron microscopy (SEM). For SEM analysis, the films were sectioned into circular samples with a diameter of 8 mm. These samples were fixed to SEM stubs using double-sided carbon tape and subsequently coated with gold in a vacuum environment to enhance conductivity. The SEM examinations were conducted at the LAMARX laboratory (UNC-CONICET, Argentina) using a Carl Zeiss Sigma microscope (Oberkochen, Germany). Images were captured at a magnification of  $2000\times$  and  $5000\times$ , utilizing an aperture size of  $30\text{ }\mu\text{m}$  and an electron high voltage (EHT) of 3 kV.

### Moisture content and total soluble matter of films

The moisture content (MC) and total soluble matter (TSM) of the PEC-based films were assessed following the methodology outlined by Zoratti *et al.*<sup>14</sup> To determine the MC, circular pieces of each film were initially weighed ( $W_0$ ) on glass plates, then oven-dried at  $110\text{ }^\circ\text{C}$  for 24 hours, and subsequently reweighed ( $W_i$ ). The MC was calculated using the following equation and performed in triplicate:

$$\text{MC\%} = [(W_0 - W_i)/W_0] \times 100 \quad (1)$$

For the TSM evaluation, each film piece initially weighed as  $W_0$  was submerged in a beaker containing 30 mL of distilled water for 24 hours, then dried at  $110\text{ }^\circ\text{C}$  for another 24 hours, after which the final weight ( $W_f$ ) was recorded. The TSM was also determined in triplicate using the following formula:

$$\text{TSM\%} = [(W_i - W_f)/W_i] \times 100 \quad (2)$$

the initial dry mass ( $W_i$ ) used for the TSM calculation was derived from the MC measurements of a similarly weighed film piece. To prevent the potential formation of thermal cross-links due to heating before water immersion, different film samples were utilized for initial and soluble dry matter assessments.

### Swelling assay

The water uptake capacities of the samples were quantified using a method outlined by Mercadal *et al.*<sup>15</sup> The water uptake percentage ( $S\%$ ) is calculated with the formula:

$$S\% = [(W_s - W_0)/W_0] \times 100 \quad (3)$$

here,  $W_0$  is the initial weight of the sample, and  $W_s$  is the weight after soaking in 30 mL of deionized water for designated periods at room temperature. After immersion, the samples are removed, and the surface is dried with tissue paper to eliminate any excess water. The test was conducted in triplicate to ensure the accuracy and reproducibility of the results.

### Water vapor permeability

Circular PEC-based film samples, each measuring  $3.14\text{ cm}^2$  and devoid of defects such as cracks, bubbles, or pinholes, were securely sealed onto the openings of aluminum permeation cups (2.0 cm diameter, 2.5 cm depth) containing anhydrous calcium chloride. The films were attached using silicone vacuum grease and a retention ring, ensuring the side was initially in contact with the casting plate faced inward. The assemblies were then placed in a humidity chamber maintained at 70% RH. Hourly weight measurements of the cups were performed until seven consistent data points were collected.

Water vapor transmission rate (WVTR, in  $\text{g m}^{-2}\text{ day}^{-1}$ ) and water vapor permeability (WVP, in  $\text{g m}^{-1}\text{ s}^{-1}\text{ Pa}^{-1}$ ) were calculated from these data according to ASTM.<sup>20</sup> The equations used were:

$$\text{WVTR} = F/A \quad (4)$$

$$\text{WVP} = (\text{WVTR} \times e)/S_p \times (\text{RH}_1 - \text{RH}_2) \quad (5)$$

where  $F$  is the slope of the linear regression of mass against time ( $\text{kg s}^{-1}$ ),  $A$  is the test area,  $e$  is the film thickness (m),  $S_p$  is the saturation vapor pressure at  $30\text{ }^\circ\text{C}$ , and  $\text{RH}_1 - \text{RH}_2$  is the difference in relative humidity between the inside of the cup (0%) and the chamber (70%).

### Mechanical properties of films

The mechanical properties of the PEC-based films were evaluated through tensile testing in accordance with the ASTM D882-02 standard.<sup>21</sup> The films were cut into bone-shaped specimens using a steel template, with a total length of 6 cm, a width of 1 cm at the ends, and 0.3 cm at the narrow central region (fracture zone). The gauge length was 4 cm, leaving 1 cm at each end for clamping. Tensile tests were conducted using an Instron universal testing machine (model EMIC 23-5S, Norwood, USA) equipped with a 50 N load cell, at a cross-head speed of  $25\text{ mm min}^{-1}$ , corresponding to a strain rate of approximately  $1\text{ s}^{-1}$ . The experiments included both freshly prepared films and those aged for two months under ambient conditions, allowing for the evaluation of mechanical durability over time.

From the stress *vs.* strain data collected during these tests, key mechanical properties such as tensile strength, elongation at break, and modulus of elasticity were calculated. Additionally, the toughness of the films was quantified by integrating the area under the stress-strain curves up to the fracture point, using the formula:

$$\text{Tensile toughness} = \int_0^{\varepsilon_f} \sigma_e \text{d}\varepsilon_e \quad (6)$$

where  $\sigma_e$  is the stress ( $\text{N m}^{-2}$ ),  $\varepsilon_e$  is the strain (unitless), and  $\varepsilon_f$  is the fracture strain of the sample, respectively.

### Degradation under soil burial conditions

The biodegradation tests for the PEC-based films were carried out following the procedure outlined by Molina Torres *et al.*<sup>22</sup>



Initially, equal masses of each film type were cut into rectangular pieces and dried at 105 °C for 12 hours, after which they were weighed to establish their initial mass ( $W_0$ ). These samples were then covered with plastic mesh to allow access to moisture and microorganisms while enabling easy retrieval and buried in soil for 20 days. The controlled environment for this experiment maintained a temperature of (23 ± 2) °C and relative humidity of (55 ± 3%), with periodic watering to ensure consistent soil moisture, which was measured gravimetrically using standard oven-drying methods. At the end of the experiment, the samples were excavated, gently cleaned to remove soil particles, dried again at 105 °C for 12 hours, and weighed ( $W_t$ ). The average weight loss was calculated to assess the biodegradation rate, using the following formula:

$$\text{Weight loss (\%)} = [(W_0 - W_t)/W_0] \times 100 \quad (7)$$

All measurements were repeated in triplicate to ensure the reliability of the data.

### *In vitro* antioxidant activity of films

Film samples were cut into 100 mg pieces for analysis of their antioxidant capacity using the 2,2-diphenyl-1-picrylhydrazyl (DPPH) radical scavenging activity assay. Each piece was submerged in 10 mL of a  $1 \times 10^{-4}$  M DPPH solution in 99.5% absolute ethyl alcohol. After an hour of incubation in the dark, the absorbance of the solution was measured at 517 nm using a Shimadzu 1800 spectrophotometer. A calibration curve was established using Trolox, ranging from 1.6 to 30 μM, to calculate the activity. The results were expressed as μmol Trolox equivalents (μmol TE) per gram of sample. Additionally, the DPPH scavenging activity percentage was calculated using the following equation:

$$\text{DPPH scavenging activity (\%)} = [(A_c - A_s)/A_c] \times 100\% \quad (8)$$

where  $A_s$  is the absorbance of the sample, and  $A_c$  is the absorbance of the control, which contains only the DPPH solution in ethanol at 517 nm. This method allows for a direct comparison of antioxidant capacities with other studies in the literature.

### *In vitro* antibacterial activity of films

The antibacterial activity of the PEC-based films was evaluated using the agar diffusion method according to Mercadal *et al.*<sup>23</sup> In this assay, the bacterial strains tested were *Escherichia coli* ATCC 25922 (*E. coli*) and *Staphylococcus aureus* ATCC 25923 (*S. aureus*). The films were prepared into 8 mm diameter discs and placed in sterilized glass Petri dishes using sterilized forceps. These discs were then positioned on agar plates that had been previously inoculated with the bacterial strains, all within a laminar airflow chamber to maintain sterility. After placing the films, the plates were incubated at room temperature for 48 hours. Post-incubation, the zones of inhibition, indicating areas where bacterial growth was prevented around

each film disc, were measured. These measurements were recorded in triplicate for each type of film.

### Antioxidant activity of films on chia oil

To assess the antioxidant effect of the PEC-based films on real foods, we selected oil rich in polyunsaturated lipids as chia oil as a representative food sample. Briefly, rolled rectangular films of 5 × 3.5 cm were placed inside khan tubes covering their inner surface, and 3 grams of oil was added to the tube. An accelerated stability test was conducted to assess the oxidative stability of oils with and without film. Each treatment, prepared in triplicate, was placed in a forced air oven at 40 ± 1 °C for 25 days according to Bordón *et al.*<sup>24</sup> Samples were periodically removed to evaluate lipid oxidation.

To determine the stability of the oil the hydroperoxide value (HPV) and induction period (IP) determined by Rancimat were carried out. HPV assay was determined following the methodology of Gimenez *et al.*<sup>25</sup> Briefly, 0.20 ± 0.01 g of oil was weighed, and 3 mL of acetic acid : chloroform (3 : 2% v/v) was added and stirred vigorously until complete dissolution was achieved. Afterwards, 0.5 mL of saturated potassium iodide solution was added and the system was kept in the dark for 1 min. The reaction was stopped by the addition of 3 mL of distilled water, and 0.5 mL of starch solution (1%, w/v) was added as an indicator. Finally, solutions were titrated with 0.001 N Na<sub>2</sub>SO<sub>3</sub> until the brown color disappeared. The calculation of HPV was carried out using eqn (10) and expressed in meqO<sub>2</sub> kg<sup>-1</sup> oil as follows:

$$\text{HPV} = (S - B) \times N \times 1000/w \quad (9)$$

where  $S$  represents the volume (mL) of the sodium thiosulfate solution consumed by the sample,  $B$  is the volume (mL) consumed by the blank,  $N$  is the normality of sodium thiosulfate solution, and  $w$  represents the mass of oil (g).

For the IP determinations, we have followed the methodology of Molina Torres *et al.*<sup>22</sup> The oxidative stability of oil samples was subjected to accelerated oxidation conditions in a Rancimat (METROHM, Switzerland) apparatus. The samples were exposed to elevated temperatures at constant airflow, and the volatile oxidation products (mostly derived from formic acid) were transferred by the airflow to the solution (distilled water). From a continuous recording of the conductivity of this solution, oxidation curves were plotted and their inflection point was defined as the induction time (IT), which was expressed in hours. The test conditions were 100 °C temperature, 20 L h<sup>-1</sup> airflow, and 1.5 g of oil.

### Permeability of oil

The oil permeability assay for the PEC-based films was conducted as described by Amariei *et al.*<sup>26</sup> In this procedure, glass vials with a capacity of 10 mL, each containing 3 mL of chia oil, were sealed using the films. These vials were then inverted and placed on filter paper, which had been weighed beforehand. This setup was maintained in a desiccator at room temperature for five days. At the end of this period, the filter



paper was weighed again to ascertain any oil leakage through the films. The percentage of oil permeated was calculated using the following equation:

$$\text{Oil\%} = [(W_s - W_0)/W] \times 100 \quad (10)$$

where  $W_0$  is the initial weight of the filter paper and  $W_s$  is the weight after 5 days.  $W$  is the weight of the 3 mL of used oil. All of the measurements were performed in triplicate.

### Statistical analysis of data

The statistical analysis of the experimental data was conducted using analysis of variance (ANOVA) to evaluate the significance of differences among group means across multiple test groups. Additionally, the unpaired *t*-test was employed to compare means between the two groups specifically. The differences were considered statistically significant if the *p*-value was less than or equal to 0.05.

## Results and discussion

### Preparation and characterization of NAES

As shown in Fig. 1A, the prepared ChClCA and ChClTA NAES are homogeneous liquids at room temperature. ChClCA exhibits an orange/yellow color attributable to the presence of CA

while ChClTA displays a brown color given by TA. The proposed molecular interactions highlighted by dashed lines display the H-bonding within the NAES systems. In both NAES, ChCl acts as an HBA forming H-bonds with CA and TA.

FTIR spectroscopy was employed to identify the main vibrational modes of NAES, as shown in Fig. 1B and C. Black arrows in the spectra point out the most relevant vibrational modes to be analyzed. The spectrum of ChCl (black line) shows the O-H stretching mode centered at  $3325\text{ cm}^{-1}$ , a broad peak at  $1634\text{ cm}^{-1}$  indicative of H-O-H bending from moisture, a common feature in hygroscopic materials, along with C-H bending at  $1478\text{ cm}^{-1}$ , and C-O stretching and C-O-H bending vibrations appearing at  $1084\text{ cm}^{-1}$  and  $1052\text{ cm}^{-1}$ , respectively.<sup>27</sup> The CA spectrum (Fig. 1B, blue line) features a broad O-H stretching at  $3295\text{ cm}^{-1}$  with peaks at  $1747\text{ cm}^{-1}$  and  $1683\text{ cm}^{-1}$  corresponding to the asymmetric and symmetric C=O stretching of carboxylic groups.<sup>28</sup>

Notably, the ChClCA spectrum (Fig. 1B, pink line) shows that the O-H band (ranging from  $3600$  to  $3100\text{ cm}^{-1}$ ) is both more intense and broader than in the individual components. The double peaks of CA at  $1747$  and  $1683\text{ cm}^{-1}$  are red-shifted to  $1753$  and  $1685\text{ cm}^{-1}$  after ChClCA formation.

For the TA spectrum (Fig. 1C, red line), a broad band at  $3255\text{ cm}^{-1}$  is observed, which is characteristic of the multiple O-H groups in this polyphenol. The distinct bands at

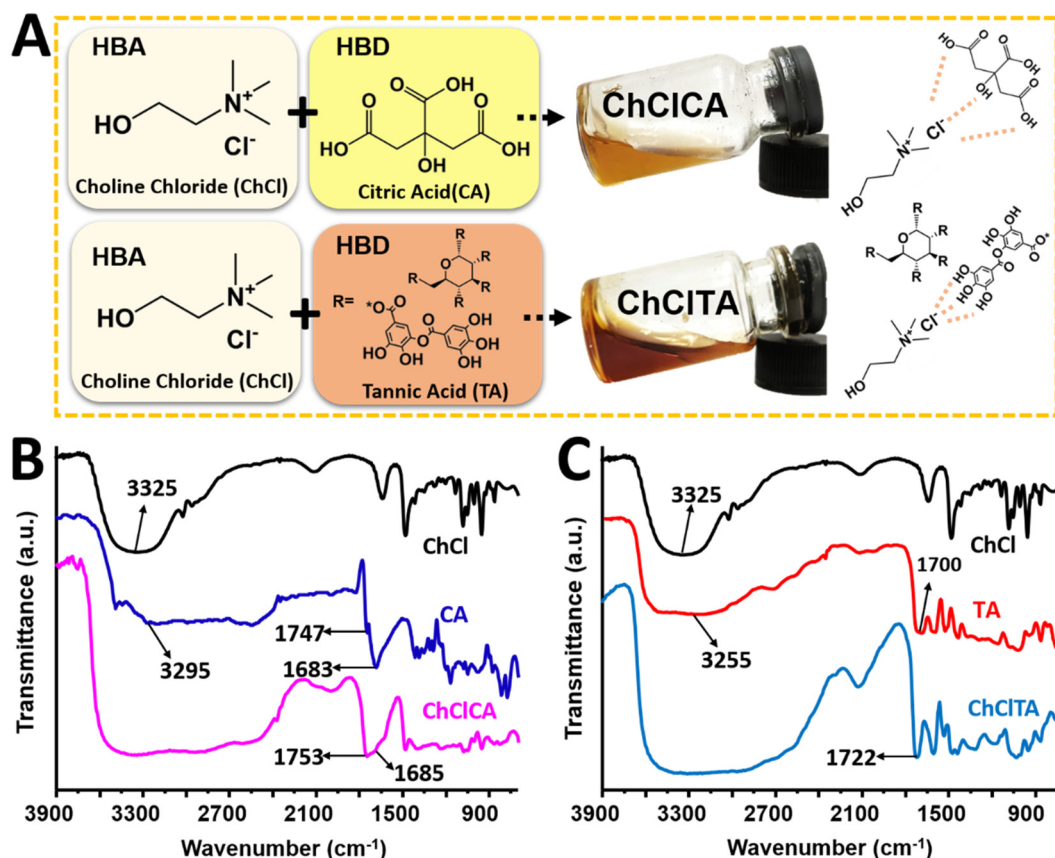


Fig. 1 (A) Schematic illustrations of the HBD and HBA compounds involved in NAES preparation, photographs of the prepared solvents and scheme of their formation. (B) FTIR spectra of C, CA and ChClCA. (C) FTIR spectra of C, TA, ChClTA.



1700  $\text{cm}^{-1}$  and 1605  $\text{cm}^{-1}$  are attributed to C=O and C=C stretching vibrations within the aromatic rings.<sup>29</sup> Similar to ChClCA, the ChClTA spectrum (Fig. 1C, sky blue line) shows an intensified and broader O-H band than seen in the pure components, with a noticeable red shift in the C=O stretching peak from 1700  $\text{cm}^{-1}$  to 1722  $\text{cm}^{-1}$  in the ChClTA NAES.

These highlighted spectral features for both NAES indicate the formation of intermolecular H-bonds in the solvents and confirm their successful preparation, in line with other works.<sup>14,15</sup>

### Preparation of films and first evaluations

As is displayed in Fig. 2A, the casting method was employed to prepare the PEC-based films incorporating the NAES in a single-step process. A selected image of a PEC-based film containing 400 wt% of ChClCA NAES (based on PEC), which displays the yield of a flexible and homogeneous material cross-linked *via* H-bonds, is shown in Fig. 2B.

Initially, the optimal amount of NAES incorporated into PEC-based films was determined through a qualitative swelling

assay using distilled water, considering that the primary limitation of PEC is its high hydrophilicity and solubility, an important characteristic from a practical standpoint in food packaging materials. As shown in Fig. 2C, PEC-based films containing 50, 100, 200, and 400 wt% of ChClCA were immersed in distilled water. After 30 minutes of exposure, the films with 200 and 400 wt% NAES demonstrated superior shape retention compared to the others, indicating a stronger resistance to water uptake which is crucial for maintaining their structural integrity in humid environments. Similar results were observed for PEC-based films containing ChClCA NAES. On the other hand, films with more than 400 wt% NAES became sticky, rendering them unsuitable for food packaging applications due to compromised material handling and performance.

Based on the above results, PEC-based films containing 200 and 400 wt% of NAES or glycerol (control films) were selected for further studies. These films are designated as "PEC", followed by the acronym of the HBD of the used NAES, and ending with the number "2" or "4", indicating whether 200 or

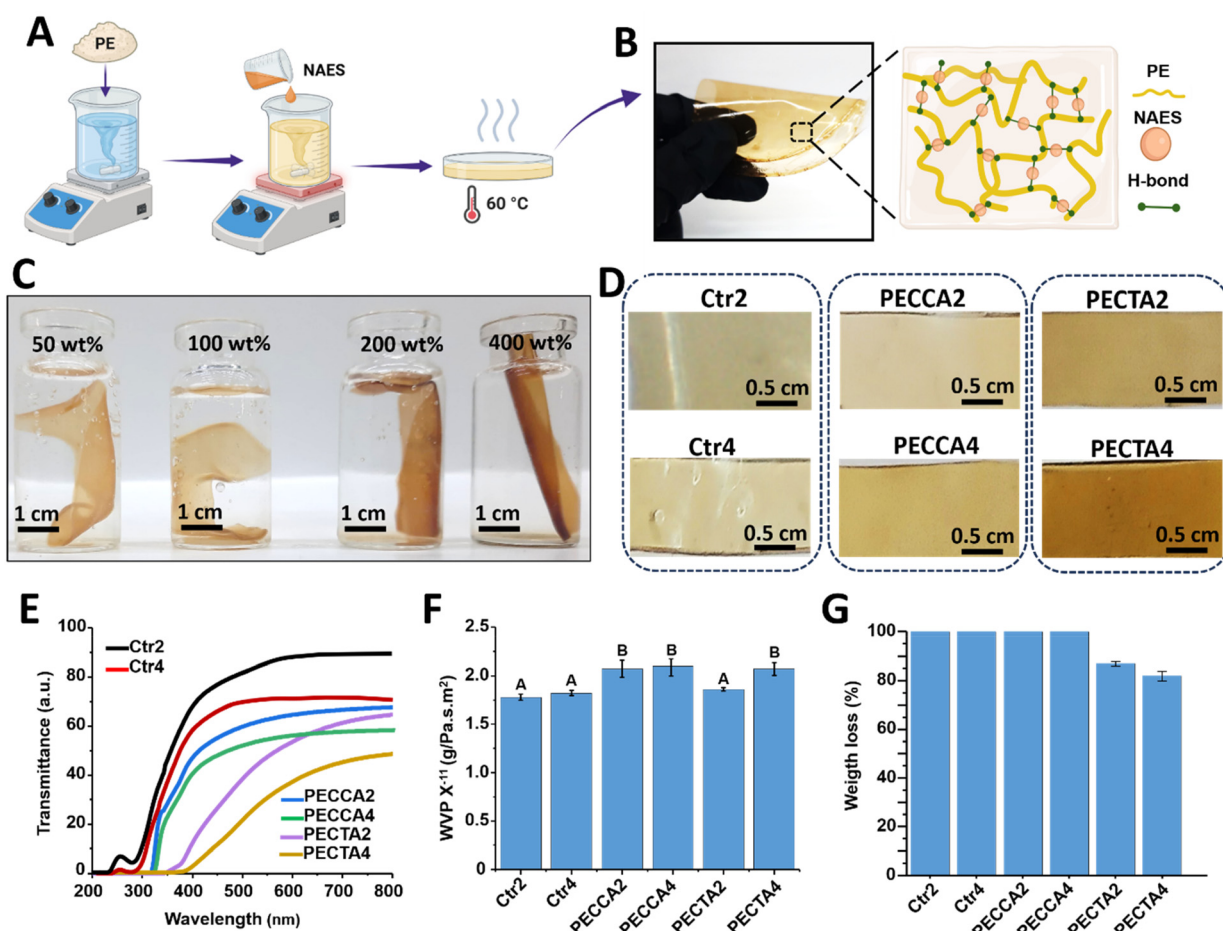


**Fig. 2** (A) Scheme of the preparation of PEC-based films. (B) Representative photography of PEC-based film using 400 wt% of CHClCA NAES, and possible crosslinked mechanism. (C) Photographs of PEC-based films containing different wt% of ChClCA NAES after the addition of distilled water. (D) Photographs of as-prepared PEC-based films containing 200 and 400 wt% of glycerol or NAES. (E) UV-visible transmission spectra of PEC-based films. (F) WVP values of as-prepared PEC-based films. (G) Weight loss (%) of PEC-based films after being buried for 20 days.



400 wt% of NAES, respectively, was incorporated. For example, films with 200 wt% and 400 wt% of ChClTA NAES are labeled PECTA2 and PECTA4, respectively. Similarly, PEC-based films containing glycerol, serving as control samples, are named Ctr2 and Ctr4 for 200 wt% and 400 wt% glycerol, respectively.

Fig. 2D presents photographs of the prepared PEC-based films, illustrating the impact of various NAES concentrations and their inherent color properties on film appearance. Initial inspection reveals that all films display a uniformly colored appearance, suggesting effective distribution of glycerol or NAES within the PEC matrix. Ctr2 and Ctr4 maintain a light color across concentrations, attributable to the colorlessness of glycerol and the slight yellowness of PEC. The films containing NAES, PECCA2 and PECCA4 appear dusky yellow due to the combination of PEC and CA. PECTA2 and PECTA4 exhibit a medium brown color, intensifying at 400 wt% ChClTA, highlighting the influence of TA and the increased concentration of ChClTA NAES.

Light-blocking properties of a film can be particularly beneficial in preventing the photooxidation of light-sensitive foods, thereby enhancing their preservation. The transmittance values between 200 and 800 nm for the PEC-based films are displayed in Fig. 2E. Notably, all PEC-based films with NAES exhibit excellent light barrier properties in the UVB region (280–320 nm), attributable to the absorption characteristics of TA<sup>30</sup> and CA,<sup>31</sup> which have absorption bands centered around 270 nm. In contrast, both controls display a peak centered at 280 nm, indicating lesser UVB-blocking properties than the PEC-based films with NAES. Furthermore, blocking properties in the UVA region (320–400 nm) increase with increasing the NAES content. In addition, the blocking properties for samples with 400 wt% of NAES or glycerol follows the next order: PECTA4 > PECCA4 > Ctr4. The same trend is observed for samples with 200 wt% of NAES or glycerol. This sequence highlights the significant impact of phenolic TA, providing the strongest UV protection. These findings also suggest that these films are effective barriers against ultraviolet light.

Concerning light blocking in the visible region, opacity values were calculated from the visible spectra and thickness of each sample (Table 1). The opacity measurements reveal a notable increase in PECTA2 and PECTA4, with values of approximately 0.20 a.u.  $\mu\text{m}^{-1}$ , compared to the control films,

**Table 1** Opacity and thickness of PEC-based films. Data are expressed as the mean  $\pm$  SD

Sample	Opacity (a.u. $\mu\text{m}^{-1}$ )	Thickness ( $\mu\text{m}$ )
Ctr2	0.10 $\pm$ 0.04 <sup>A</sup>	401.7 $\pm$ 34.2 <sup>A</sup>
Ctr4	0.11 $\pm$ 0.02 <sup>A</sup>	726.7 $\pm$ 21.9 <sup>B</sup>
PECCA2	0.09 $\pm$ 0.03 <sup>A</sup>	459.0 $\pm$ 27.3 <sup>A</sup>
PECCA4	0.10 $\pm$ 0.02 <sup>A</sup>	763.0 $\pm$ 28.0 <sup>B</sup>
PECTA2	0.19 $\pm$ 0.03 <sup>B</sup>	457.0 $\pm$ 39.7 <sup>A</sup>
PECTA4	0.20 $\pm$ 0.02 <sup>B</sup>	690.3 $\pm$ 38.6 <sup>B</sup>

Significant differences ( $P < 0.05$ ) are indicated by different letters in the same column.

which exhibit lower opacity at around 0.10 a.u.  $\mu\text{m}^{-1}$ . This increased opacity in PECTA films is attributed to the high concentration and brown color of TA. In contrast, PECCA2 and PECCA4 films, which show opacity values of  $0.09 \pm 0.03$  a.u.  $\mu\text{m}^{-1}$  and  $0.10 \pm 0.02$  a.u.  $\mu\text{m}^{-1}$  demonstrating the poor blocking properties of CA given by their subtle yellow color.

Water barrier properties are another feature crucial in food packaging to preserve high-moisture foods and ensure stability and quality during processing and storage. The water vapor permeability (WVP) results shown in Fig. 2F display low values for all PEC-based in the range of  $1.75\text{--}2.25 \times 10^{-11}$  g Pa  $\text{s}^{-1}$   $\text{m}^{-2}$ . These low WVP values are indicative of high structural integrity and effective barrier properties within the film matrix. The integrity and performance of these films are likely due to the homogeneous distribution and NAES throughout the material, contributing to a uniform barrier against moisture ingress. This uniform distribution helps to minimize the presence of microvoids or discontinuities in the film, which can significantly enhance vapor permeability. Notably, the low WVP values observed are lower compared to similar studies involving PEC<sup>32–34</sup> or NAES.<sup>35,36</sup> For context, the WVP values obtained for our PEC-based films are consistent with or lower than those reported for other biopolymer-based films. Starch films, for instance, typically exhibit WVP values in the range of  $10^{-10}$  to  $10^{-11}$  g Pa $^{-1}$   $\text{s}^{-1}$   $\text{m}^{-2}$ , depending on the formulation and plasticizer content.<sup>37</sup> In contrast, conventional synthetic packaging materials such as low-density polyethylene (LDPE), generally present WVP values in the order of  $10^{-14}$  g Pa $^{-1}$   $\text{s}^{-1}$   $\text{m}^{-2}$ , offering superior moisture barrier properties.<sup>38</sup>

The biodegradability of PEC-based films was assessed to confirm their suitability as eco-friendly food packaging. Samples were buried in soil and their weight loss was documented after 20 days. As illustrated in Fig. 2G, all PEC-based films exhibited substantial biodegradation, with weight loss exceeding 80%, confirming their high biodegradability. Notably, the control films exhibited complete (100%) weight loss, whereas films containing TA-based NAES showed an average weight loss of approximately 80%. This indicates that the extensive crosslinking induced by polyphenols such as TA contributes to the formation of a more stable network structure, which may, in turn, slow the biodegradation process. Furthermore, consistent with previous findings, crosslinking in polymeric films has been shown to reduce water absorption capacity (as discussed in the following section), thereby limiting internal moisture availability, an essential factor for the microbial activity that drives biodegradation.<sup>20,39–41</sup>

## Physicochemical properties of the films

Chemical characterization of PEC-based films was performed through the acquisition of FTIR spectra to elucidate changes in the PEC matrix. As displayed in Fig. 3A, the Ctr2 spectrum reveals a broad O–H stretching vibration band centered at 3265  $\text{cm}^{-1}$ . Additionally, the peaks at 1750  $\text{cm}^{-1}$  and 1647  $\text{cm}^{-1}$  are indicative of C=O stretching vibrations associated with methyl-esterified carboxyl and carboxyl groups in PEC, respectively. A further peak at 1440  $\text{cm}^{-1}$  is linked to the



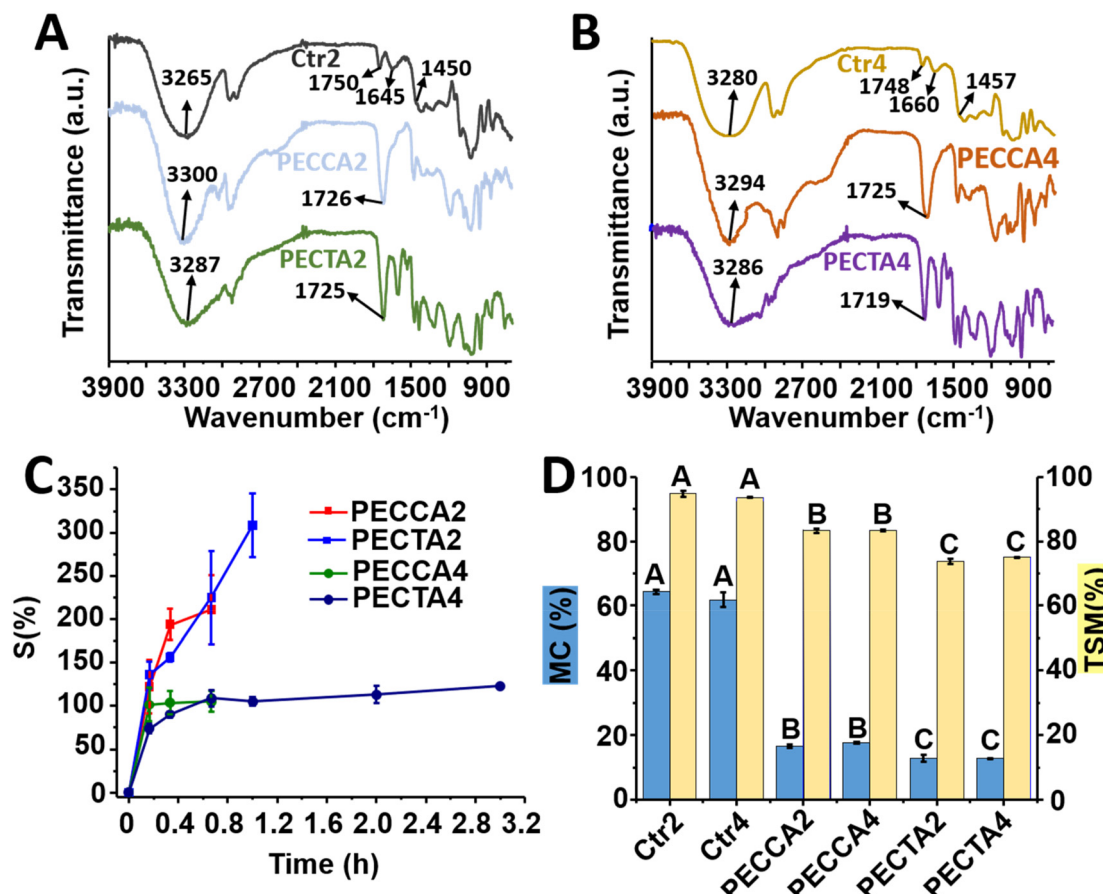


**Fig. 3** (A) FTIR spectra of PEC-based films with 200 wt% of NAES or glycerol. (B) FTIR spectra of PEC-based films with 400 wt% of NAES or glycerol. (C) Swelling behavior of PEC-based films with 200 and 400 wt% of NAES. (D) Moisture content (MC) and total soluble matter (TSM) values of PEC-based films. Values within the same color bar not followed by different letters are statistically similar ( $p \geq 0.05$ ) according to the Tukey test.

symmetric stretching vibration of the  $-\text{COO}-$  group. Peaks at  $2935\text{ cm}^{-1}$  and  $2886\text{ cm}^{-1}$  represent C-H bending, and the peak at  $1019\text{ cm}^{-1}$  is attributed to the C-O-C stretching in the saccharide structure of PEC.<sup>9,42</sup>

Upon comparing the FTIR spectra of PECCA2 and PECTA2 with Ctr2 (Fig. 3A), it is noted that the band for O-H stretching vibrations becomes stronger, wider, and shifts from  $3265\text{ cm}^{-1}$  in Ctr2 to  $3300\text{ cm}^{-1}$  and  $3287\text{ cm}^{-1}$  in PECCA2 and PECTA2, respectively. Similarly, the C=O stretch at  $1750\text{ cm}^{-1}$  shows a blue shift to approximately  $1725\text{ cm}^{-1}$  in films containing 200 wt% NAES. In the same line, comparing the FTIR spectra of PECCA4 and PECTA4 with Ctr4 (Fig. 3B) the O-H stretching vibration mode is more intense, broader, and red-shifted in the films with the NAES. Specifically, the peak shifts from  $3280\text{ cm}^{-1}$  (Ctr4) to  $3294$  and  $3286$  for PECCA4 and PECTA4 films, respectively. The C=O vibrational mode at  $1748\text{ cm}^{-1}$  in the Ctr4 spectrum also shifts to  $1725\text{ cm}^{-1}$  and  $1719\text{ cm}^{-1}$  in PECCA4 and PECTA4, respectively.

These shifts in spectral peaks, whether blue or red, indicate the formation of new hydrogen bonds and other non-covalent interactions between the NAES and the PEC matrix. Polyphenols such as TA have been reported to facilitate non-

covalent crosslinking with diverse biopolymers<sup>43</sup> and polysaccharides, including PEC,<sup>44–47</sup> leading to spectral shifts comparable to those observed here. Moreover, organic acids such as CA have also been shown to participate in physical crosslinking with PEC.<sup>48,49</sup>

Water uptake behavior is critical for evaluating PEC-based films for food packaging. Fig. 3C illustrates the swelling behavior of the materials, highlighting their capacity to reach maximum swelling percentages (S%). Both control films have rapid water uptake reaching a dissolving value at 0.2 h aligning with the findings by other authors,<sup>9,50</sup> so the solubility of these controls cannot be tested. Notably, PEC-based films with NAES exhibit significantly improved water uptake resistance, enduring up to 3 hours of water immersion, which is 15 times more than the duration of the control films. Specifically, PECTA2 and PECTA4 show remarkable endurance, with S% values of 300% and 125% after 1 hour and 3 hours of immersion, respectively. These findings align with the FTIR results, supporting the formation of a crosslinked network within the PEC matrix, particularly for TA-based NAES. Similarly, PEC-based films containing CA demonstrate superior water resistance compared to the control films, also indicating the

effective formation of a crosslinked network within the PEC matrix. Additionally, films containing 400 wt% NAES display enhanced swelling resistance compared to those with 200 wt%, attributed to the higher solvent concentrations which increase TA and CA presence, resulting in a denser and more robust crosslinked network, in line with other reports.<sup>14,15</sup>

These results demonstrate that the swelling performance of our films is on par with the leading examples in recent literature, as PEC-based films crosslinked with vanillin and  $\text{Fe}^{3+}$ <sup>9</sup> or  $\text{CaCl}_2$ <sup>34</sup> which report swelling percentages around 1000% over significantly shorter immersion times. This performance underscores the effectiveness of NAES in enhancing the water uptake resistance of PEC-based films, a traditional weak link that limits their use in food packaging.

Consistent with the swelling behavior, films incorporating NAES demonstrate reduced moisture content (MC) compared to controls, as illustrated in Fig. 3D (blue bars). This reduction in MC likely results from the crosslinking effect of NAES, which limits water penetration into the films. Additionally, the total soluble matter (TSM) values shown in Fig. 3D (yellow bars) corroborate this observation. The TSM data clearly show that films with NAES have consistently lower solubility than the control films, following the same trend observed for swelling assays.

### Morphological characterization of the films

The SEM analysis of PEC-based films reveals diverse surface morphologies that significantly reflect the structural and chemical modifications resulting from various concentrations and types of NAES used in their formulation. As shown in Fig. 4A, the surface of Ctr2 displays roughness, consistent with other studies on PEC-based films using glycerol as a plasticizer.<sup>51,52</sup> In turn, Ctr4 exhibits a smoother surface relative to Ctr2, due to the increased amount of glycerol, which enhances the surface integrity and uniformity of the material through its plasticizing effect.

The inclusion of 200 wt% ChClCA and ChClTA NAES, as shown in Fig. 4C and E respectively, reveals a marked improvement in surface texture compared to the Ctr2. These films exhibit smoother surfaces with some folds but are free from pores or cracks, which illustrates the effective plasticizing impact of NAES and their seamless integration into the PEC matrix. At higher concentrations (400 wt%), shown in Fig. 4E and F, this smoothing effect is more pronounced, indicating a denser and homogeneous network. This is consistent with the film's swelling properties, where higher NAES concentrations, linked to enhanced crosslinking, contributed to reduced water uptake. Interestingly, compared to soy protein films with the same NAES,<sup>15</sup> these PEC-based films exhibit better and more uniform distribution, leading to a smoother surface. This highlights how NAES modifies the microscale structure of films depending on the matrix type, whether protein or polysaccharide, which significantly impacts their macroscopic properties.

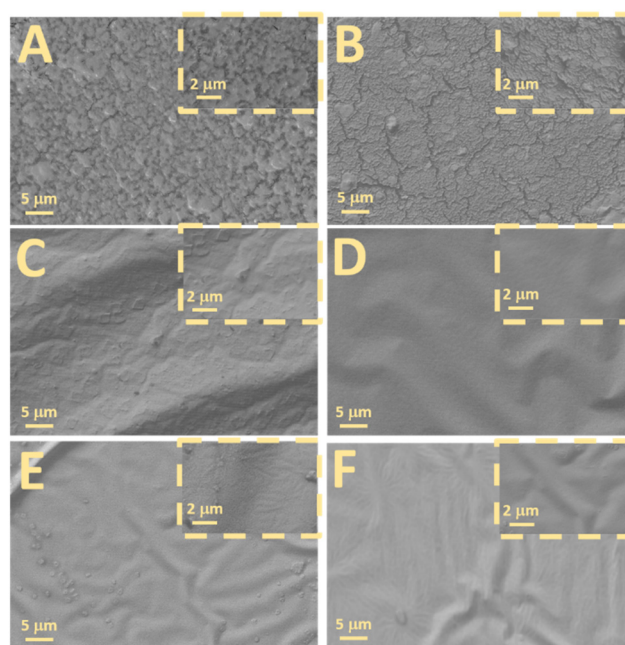


Fig. 4 SEM images of Ctr2 (A), Ctr4 (B), PECCA2 (C), PECCA4 (D), PECTA2 (E) and PECTA4 (F) films.

### Mechanical properties of films

Strain *vs.* stress curves displayed in Fig. 5A and B highlight the mechanical behavior of PEC-based films with 200 and 400 wt% of NAES or glycerol. Initial observation of the curves reveals that control films exhibit higher strain values compared to films with NAES, demonstrating the significant plasticizing effect of glycerol. Notably, Ctr4, which contains a higher glycerol content, exhibits higher elongation at break (EB) than Ctr2. This result is consistent with prior findings, as plasticizers are known to improve film flexibility and stretchability while reducing tensile strength (TS) by weakening intermolecular forces between polymer chains.<sup>53</sup>

The incorporation of NAES enhances stress values in all samples relative to controls while decreasing strain, attributable to the crosslinking effects of polyphenols and CA within the NAES.<sup>54</sup> Notably, Fig. 5C (blue-sky bars) illustrates that the TS value of Ctr2 stands at  $1.25 \pm 0.08$  MPa. In comparison, the incorporation of NAES increased TS values, with PECTA2 achieving the highest strength at  $2.2 \pm 0.2$  MPa and PECCA2 showing  $1.5 \pm 0.14$  MPa. This difference between PECTA and PECCA films can be attributed to the higher number of OH groups in TA compared to CA, which facilitates more extensive hydrogen bonding and stronger interactions with the biopolymer matrix. Consequently, TA promotes the formation of a more densely crosslinked network, thereby enhancing rigidity and mechanical strength. Increasing NAES content from 200 to 400 wt% slightly reduces TS values, as evidenced by the TS of PECTA4 and PECCA4 at  $1.2 \pm 0.1$  MPa and  $1.0 \pm 0.9$  MPa, respectively. The EB values marginally decreased, for instance, from  $30.7 \pm 2.7\%$  for PECCA2 to  $27.8 \pm 3.7\%$  for PECCA4, as demonstrated in Fig. 5D (blue-sky bars). This trend is consist-



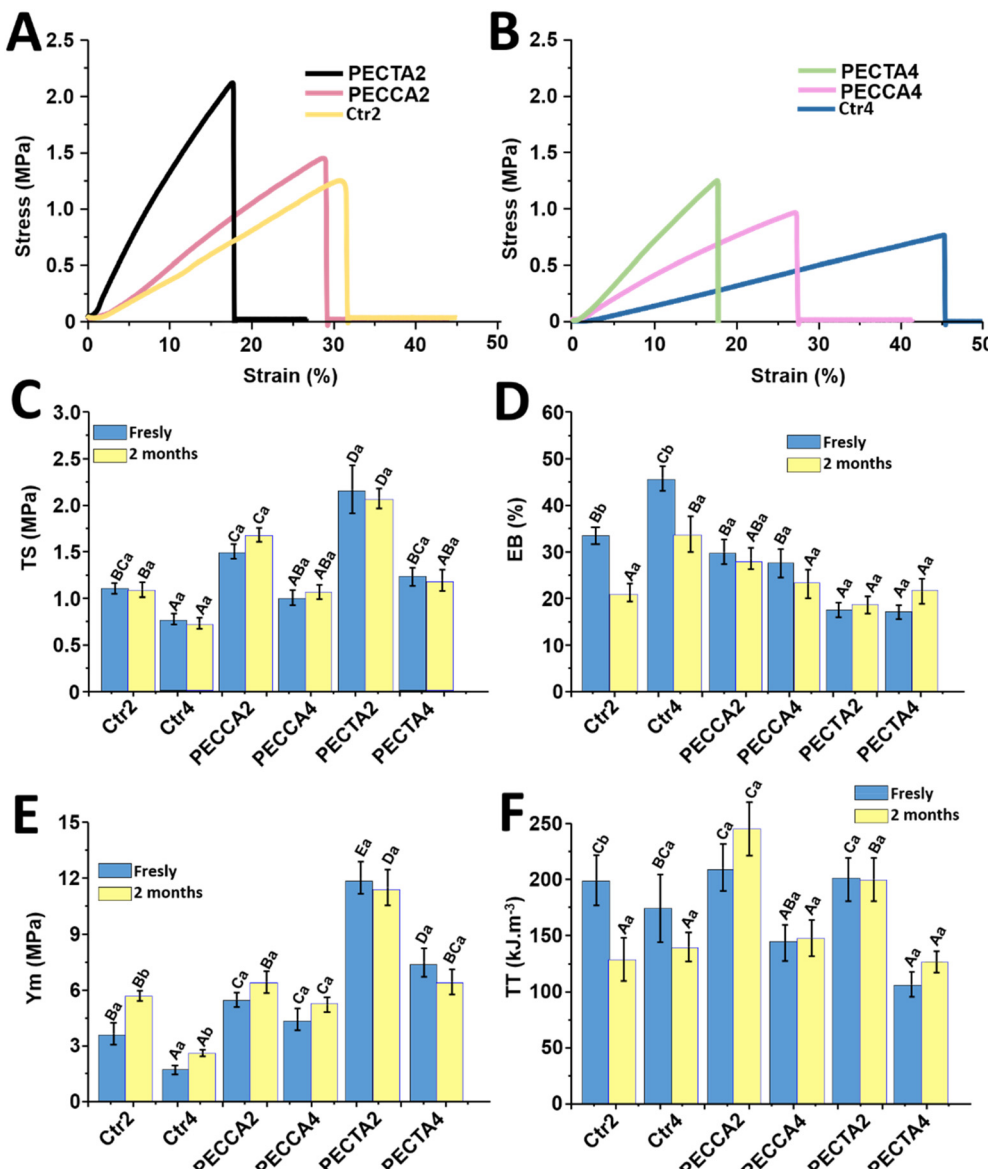


**Fig. 5** (A) Stress vs. strain curves of PEC-based films with 200 wt% of NAES or glycerol. (B) Stress vs. strain curves of PEC-based films with 400 wt% of NAES or glycerol. (C) TS values for PEC-based films measured immediately after preparation and following 2-months of storage. (D) EB values for PEC-based films measured immediately after preparation and following 2-months of storage. (E) Ym values for PEC-based films measured immediately after preparation and following 2-months of storage. (F) TT values for PEC-based films measured immediately after preparation and following 2-months of storage. Different uppercase indicates significant differences ( $p < 0.05$ ) between different samples comparing the freshly prepared or those after 2 months of storage separately. Lowercase denotes significant differences ( $p < 0.05$ ) within the same film type, comparing fresh and 2-month stored conditions.

ent across all PEC-based films when comparing 200 wt% and 400 wt% NAES formulations. The decline in mechanical properties with increasing NAES concentrations can be attributed to the antagonistic effects of plasticizing and crosslinking. Specifically, as the NAES concentration reaches 400%, the plasticizing effect becomes dominant over crosslinking, leading to a decrease in mechanical strength. Moreover, despite extensive crosslinking, the EB remains unchanged. This behavior likely results from saturation of binding sites within the PEC matrix, consistent with previous observations.<sup>15</sup>

The Young's modulus (Ym) values were higher for NAES-incorporated films than controls, aligning with the observed TS trends (Fig. 5E, sky-blue bars). Furthermore, in line with the above observations, films with 200 wt% NAES exhibit higher tensile toughness (TT) compared to those with 400 wt% NAES or glycerol, as displayed in Fig. 5F (sky-blue bars).

To further understand the durability of PEC-based films in food packaging, we examined the mechanical properties after 2 months at 25 °C (Fig. 5, yellow bars). This assessment allows

us to evaluate how well the films maintain their mechanical integrity over time.

Remarkably, all PEC-based films maintain their TS values even after 2 months of storage, as illustrated in Fig. 5C, comparing sky-blue and yellow bars. However, the EB values for Ctr2 and Ctr4 see a notable reduction, dropping from  $32.4 \pm 1.7\%$  to  $20.2 \pm 5.2\%$ , and from  $46.5 \pm 1.3\%$  to  $33.3 \pm 4.0\%$ , respectively. In contrast, EB values of PEC-based films with NAES remain relatively stable, around 20% (Fig. 5D, sky-blue *vs.* yellow bars). The reduction in EB values for the control films indicates material aging, likely due to moisture loss (as these samples show the highest MC values, shown in Fig. 3D). This observation aligns with previous findings on PEC-based films which reported decreased EB after prolonged storage.<sup>55</sup> Similar trends were observed for both Ym and TT between freshly prepared and 2-month-aged PEC films, with statistically significant differences appearing only in the control samples (Fig. 5E and F, sky-blue *vs.* yellow bars). This suggests that the crosslinked network within the NAES-enhanced PEC films is robust and dense enough to preserve mechanical properties

over time, underscoring their potential for long-term food packaging applications.

#### Antibacterial and antioxidant activity of films

Films with antioxidant and antimicrobial properties are essential for developing active food packaging that extends food shelf life. To assess these properties, the *in vitro* antioxidant and antibacterial activities of PEC-based films were evaluated using bacterial growth inhibition by diffusion in agar and DPPH assays.

As shown in Fig. 6A, control films, with a measured pH of 5, exhibited no antibacterial activity against either Gram-positive (*S. aureus*) or Gram-negative (*E. coli*) bacteria strains, consistent with previous reports.<sup>56,57</sup> In contrast, all PEC-based films with NAES demonstrated inhibition zones for both bacterial strains. NAES act by disrupting bacterial cell membranes through hydrophobic interactions, leading to leakage of essential intracellular components and bacterial death.<sup>15</sup>

The samples with 200 wt% and 400 wt% of ChClCA reached inhibition diameters, for both bacteria strains, of around 29

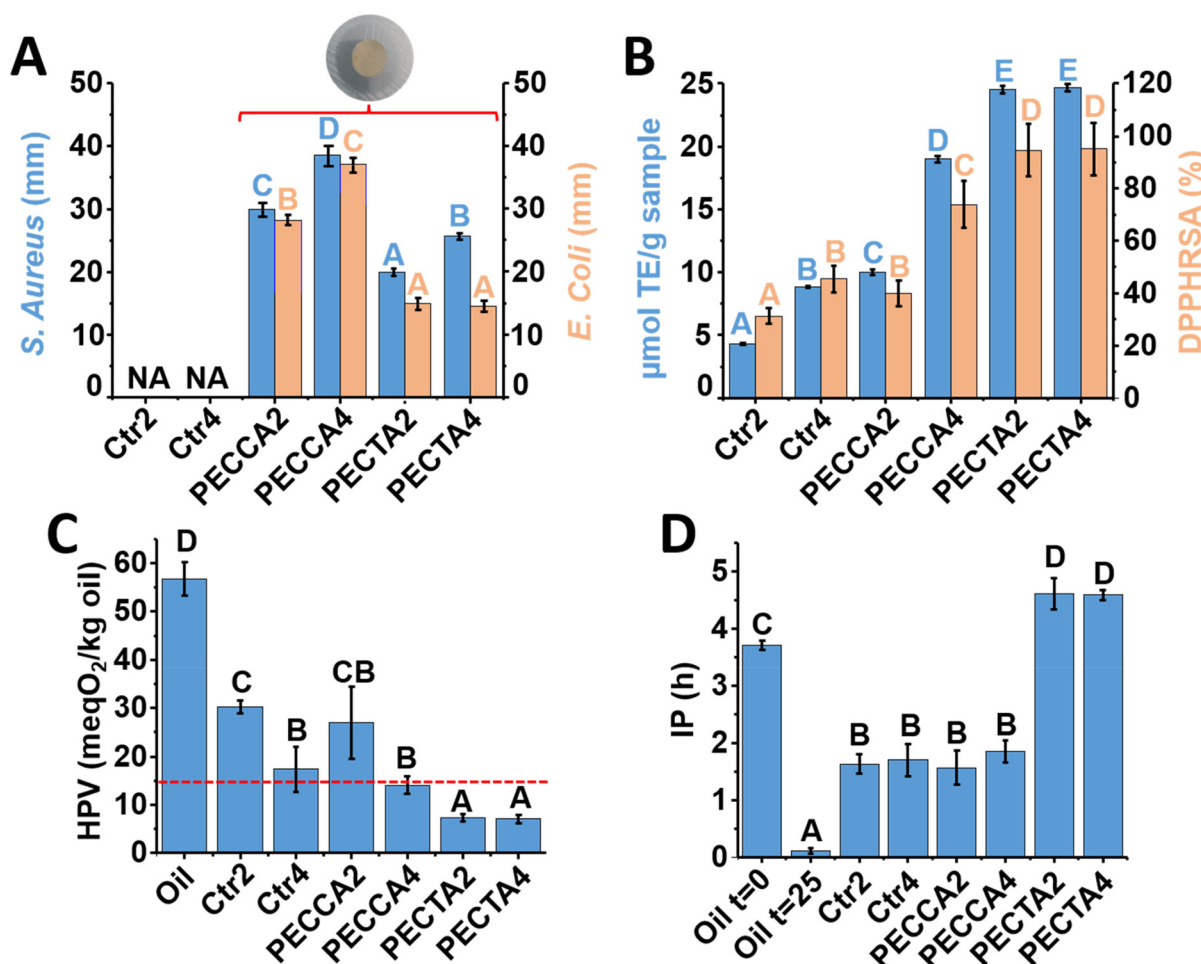


Fig. 6 (A) Inhibition zones of PE-based films against *S. aureus* and *E. coli*. (B) Antioxidant activities of the as-prepared films measured by DPPH assay. (C) HPV values on chia oil after 25 days. (D) IP values on chia oil after 25 days. Mean values in chart bars with the same letter are not significantly different ( $p \geq 0.05$ ) according to the Tukey test.



and 39 mm, respectively. As anticipated, larger inhibition diameters were observed with increasing ChClCA content, which we attribute to the elevated concentration of active components in the NAES formulation. Specifically, organic acids such as CA inhibit bacterial proliferation by integrating into the bacterial cell membrane and disrupting protein synthesis.<sup>58</sup>

PECTA2 and PECTA4 films exhibit inhibition zones of 20 mm and 25 mm, respectively, against *S. aureus*, while both films show a 15 mm inhibition diameter against *E. coli*. Here TA works as an inhibitor of the NorA efflux pump, promoting bacterial cell death.<sup>59</sup>

Notably, films incorporating ChClCA NAES demonstrated enhanced antibacterial activity compared to those with ChClTA NAES, aligning with previous findings.<sup>15</sup> Interestingly, although soy protein films containing the ChClTA NAES show no antibacterial activity against *E. coli*, PEC-based films incorporating the same eutectic mixture do exhibit notable antibacterial effects. This improved efficacy is likely due to the acidic environment provided by PEC in the presence of acidic NAES, which lowers the pH to below 2.5, enhancing the antibacterial effect.<sup>18</sup> The primary antibacterial mechanism in PEC films involves galacturonic acid, which disrupts bacterial cell walls by forming a polyelectrolyte complex with lipopolysaccharides on bacterial surfaces, thus impacting their permeability and function.<sup>60</sup> Importantly, control films without NAES show no antibacterial activity, as the presence of glycerol as a plasticizer maintains the environment at pH 5. This contrast highlights the critical role of the acidic components within NAES in activating the antibacterial properties of the PEC-based films.

Concerning the antioxidant activity of the PEC-based films, as shown in Fig. 6B, all samples demonstrated some level of activity in DPPH assays. Ctr2 and Ctr4 exhibited 4 and 9  $\mu\text{mol TE g}^{-1}$  sample, or 11% and 15% DDPHRSA, respectively. This activity is attributed to the inherent antioxidant properties of PEC, which vary depending on their source.<sup>19,61</sup> It is important to note that in our study, we used commercially available PEC without specific origin details.

Remarkably, the PEC-based films with ChClTA NAES demonstrate significantly enhanced antioxidant activities, achieving 24  $\mu\text{mol TE g}^{-1}$  sample and consistently displaying 95% DDPHRSA. This robust performance is attributed to the catechols and pyrogallol groups in TA, which effectively donate electrons to neutralize DPPH radicals, as highlighted by Kim *et al.*<sup>62</sup> In turn, the hydroxyl groups and acidifier action of CA also impart antioxidant activity, but is weaker than polyphenols.<sup>63</sup> Notably, when soy protein matrices combined with ChClTA are used to develop films, they exhibit very poor antioxidant activity.<sup>15</sup> Therefore, the combination of PEC and ChClTA presents a better prospect for extending the shelf life of food products sensitive to oxidation.

Based on previous *in vitro* antibacterial and antioxidant results, we conclude that these PEC-based films show excellent prospects for extending the shelf life of food products. So, as a proof of concept, their antioxidant properties were further investigated in real food samples.

For this, the antioxidant activity of the films was assessed in chia oil over 25 days under accelerated oxidative conditions at 40 °C. Hydroperoxide values (HPV) and induction period (IP) measurements were conducted after the storage period of all oil samples covered with the films to estimate their oxidative stability. It is important to highlight that accelerated oxidative conditions were thermally originated according to Bordón *et al.*<sup>24</sup> As depicted in Fig. 6C, after 25 days, the oil sample without any film showed an HPV of  $56.7 \pm 3.5 \text{ meqO}_2 \text{ kg}^{-1}$  oil. In comparison, control films Ctr2 and Ctr4 recorded HPVs of  $30.3 \pm 1.3$  and  $24.6 \pm 2.7 \text{ meqO}_2 \text{ kg}^{-1}$  oil, respectively, demonstrating the antioxidant activity of PEC, as corroborated by the DPPH assay. However, despite this activity, these values exceed the Codex Alimentarius limit for cold-pressed oils of  $15 \text{ meqO}_2 \text{ kg}^{-1}$  oil.<sup>64</sup> In contrast, PECCA4, PECTA2, and PECTA4 films display HPV values below this limit (Fig. 6C, dashed line), with both films incorporating ChClTA showing the lowest at  $7.5 \pm 0.7 \text{ meqO}_2 \text{ kg}^{-1}$  oil.

In line, IP results (Fig. 6D) are consistent with the conclusions from the HPV tests, underscoring the substantial impact of PEC-based films containing ChClTA NAES. Specifically, the IP for the PECTA2 and PECTA4 were  $4.61 \pm 0.28 \text{ h}$  and  $4.59 \pm 0.09$ , both significantly larger than the control and PECCA films.

From these results, we demonstrated that the films developed with ChClTA effectively inhibit oxidative deterioration, as evidenced by significantly lower HPV and extended IP measured using the Rancimat method. Regarding the films with ChClCA NAES, they exhibit antioxidant activity, attributed to the inherent antioxidant properties of PEC and the hydroxyl groups and acidifying action of CA. However, this activity is not as potent as that provided by TA.

These promising results highlight the potential of these films as a protective barrier against lipid oxidation, making them a valuable strategy for extending the shelf life of chia oil and other lipid-based food products.

Since we have demonstrated the ability of these films to protect chia oil from oxidative processes, which suggests their potential use as an oil coating material, the permeability or diffusion of oil through these films was evaluated. The qualitative test confirmed the expected results based on the hydrophilic properties of the films, showing that all PEC-based materials exhibited oil permeation values below 0.5%. This result confirms the absence of semi-macroscopic pores or cracks, ensuring effective oil barrier properties, resulting in advantageous for further antioxidant applications.

## Conclusions

In this study, biodegradable PEC-based films containing high concentrations of binary NAES, composed of ChCl and TA or CA, were prepared. The films exhibited excellent UV light-blocking properties, with PECTA4 film showing superior visible light-blocking features. The increase in the amount of NAES notably improved water resistance, with PECTA proving



to be the most effective, likely due to the denser crosslinking network formed by the synergistic interaction between TA and PEC matrix.

Mechanical properties were also enhanced in NAES-containing films, attributed to the robust molecular interactions between TA and CA with the PEC matrix. Aging tests further confirmed that PEC-based films containing NAES retained their mechanical properties over time compared to controls.

These films effectively reduce the growth of both Gram-negative and Gram-positive bacteria strains in *in vitro* assays. Moreover, they demonstrate superior antimicrobial and antioxidant performance compared to films that incorporate the same NAES in a soy protein matrix, due to the intrinsic active properties of the PEC matrix.

The films demonstrated preventing oxidation in chia oil with PECTA films showing the highest antioxidant activity, a result of the antioxidant capacities of TA, which effectively scavenge free radicals and protect chia oil samples against oxidation, maintaining HPV values below the Codex Alimentarius limit.

The simplicity of incorporating NAES into the PEC matrix without the need for complex steps enhances the production process's feasibility for industrial scaling. The findings of this study suggest that these NAES represent a viable strategy to enhance both the functional and structural properties of bio-polymer-based films. They also contribute antimicrobial and antioxidant activities, resulting in environmentally friendly materials capable of protecting and extending the shelf life of high-lipid or low-moisture foods, such as oils or avocados. This research contributes to the ongoing efforts in food science to develop more sustainable and effective packaging solutions, aligning with the green transition goals of reducing environmental impact and utilizing renewable resources more efficiently.

## Conflicts of interest

There are no conflicts to declare.

## Data availability

Data will be made available on request.

## Acknowledgements

The authors acknowledge financial support from CONICET (PIP 11220200103225CO), FONCyT (PICT 2020-1955 and PICT-2019-4265), SECyT-UNC (33620180100568CB RES 411/18) and PROIINDIT 2024 from FCA-UNC. P. G. and P. A. Mercadal acknowledge the fellowships provided by CONICET. M. L. Picchio gratefully acknowledges the financial support received from the Basque Government, Department of Education (IT1766-22), from IKERBASQUE-Basque Foundation for Science, and from the European Union under the IONBIKE 2.0

project (grant agreement n. 101129945, <https://doi.org/10.3030/101129945>). The authors are grateful for the 23-5S Instron-Emic mechanical analyzer obtained from PRIMAR-TP: 32520170100384CB and LAMARX Lab (FAMAF-UNC) for performing the SEM micrographs.

## References

- 1 S. Sinha, *Polym. Renewable Resour.*, 2024, **15**, 193–209.
- 2 S. Roy, B. Malik, R. Chawla, S. Bora, T. Ghosh, R. Santhosh, R. Thakur and P. Sarkar, *Int. J. Biol. Macromol.*, 2024, **278**, 134658.
- 3 S. Paidar, A. M. Nafchi, S. Vahedi, M. Beigi, S. A. Al-Hilifi, N. Zamindar, H. Sajadizadeh, S. Abbasi and L. Nateghi, *J. Food Meas. Charact.*, 2024, **18**, 5171–5185.
- 4 A. J. V. Singaram, S. Guruchandran and N. D. Ganesan, *Packag. Technol. Sci.*, 2024, **37**, 237–262.
- 5 L. Barrera-Chamorro, Á. Fernandez-Prior, F. Rivero-Pino and S. Montserrat-de la Paz, *Carbohydr. Polym.*, 2025, **348**, 122794.
- 6 A. Dirpan, Y. Deliana, A. F. Ainani, I. Irwan and N. A. Bahmid, *Polymers*, 2024, **16**, 2783.
- 7 S. Li, N. Wei, J. Wei, C. Fang, T. Feng, F. Liu, X. Liu and B. Wu, *Int. J. Biol. Macromol.*, 2024, **266**, 131248.
- 8 W. Yang, S. Zhang, A. Feng, Y. Li, P. Wu, H. Li and S. Ai, *Food Hydrocolloids*, 2024, **156**, 110364.
- 9 T. Qiang, W. Ren and L. Chen, *Food Hydrocolloids*, 2024, **149**, 109539.
- 10 J. Jeya Jeevahan, M. Chandrasekaran, S. P. Venkatesan, V. Sriram, G. Britto Joseph, G. Mageshwaran and R. B. Durairaj, *Trends Food Sci. Technol.*, 2020, **100**, 210–222.
- 11 S. Du, X. Chen, M. Li, B. Peng, Q. Lyu, L. Zhang and J. Zhu, Ultratough and Highly Conductive Supramolecular Poly (Vinyl Alcohol) Eutectogels via a Sequentially Enhanced Strategy, *Adv. Funct. Mater.*, 2025, **25**, 2409726.
- 12 B. Chenthama, M. Shaibuna and R. L. Gardas, in *Deep Eutectic Solvents*, Elsevier, 2025, pp. 1–26.
- 13 H. Iyer, A. Mandal, M. Holden and E. Roumeli, *RSC Appl. Polym.*, 2025, **3**, 407–419.
- 14 M. Zoratti, P. A. Mercadal, C. I. Alvarez Igarzabal, M. L. Picchio and A. González, *Int. J. Biol. Macromol.*, 2024, **283**, 137970.
- 15 P. A. Mercadal, M. L. Picchio and A. González, *Food Hydrocolloids*, 2024, **147**, 109414.
- 16 R. Castro-Muñoz, A. Can Karaç, M. Saeed Kharazmi, G. Boczkaj, F. J. Hernández-Pinto, S. Anusha Siddiqui and S. M. Jafari, *Crit. Rev. Food Sci. Nutr.*, 2024, **64**, 10970–10986.
- 17 M. H. Shafie, R. Yusof, I. Naharudin, T. W. Wong, Z. Zafarina and C.-Y. Gan, *J. Food Meas. Charact.*, 2022, **16**, 3832–3843.
- 18 R. M. Abdelgawad, N. Damé-Teixeira, K. Gurzawska-Comis, A. Alghamdi, A. H. Mahran, R. Elbackly, T. Do and R. El-Gendy, *Bioengineering*, 2024, **11**, 653.



19 J. Meerasri and R. Sothornvit, *Int. J. Biol. Macromol.*, 2020, **147**, 1285–1293.

20 ASTM, *Standard Test Methods for Water Vapor Transmission of Materials*, 2010.

21 ASTM Standard, *Standard test method for tensile properties of thin plastic sheeting (D882-02)*, West Conshohocken, PA, USA, 2002.

22 M. A. Molina Torres, P. A. Gimenez, P. A. Mercadal, C. I. Alvarez Igarzabal and A. González, *Food Hydrocolloids*, 2024, **155**, 110185.

23 P. A. Mercadal, Y. M. Martínez, M. Zoratti, M. I. Velasco, M. R. Romero, G. Tommasone, M. L. Picchio and A. González, *ACS Appl. Polym. Mater.*, 2025, **7**, 1361–1375.

24 M. G. Bordón, S. P. Meriles, P. D. Ribotta and M. L. Martínez, *J. Food Sci.*, 2019, **84**, 1035–1044.

25 P. A. Gimenez, A. Lucini Mas, P. D. Ribotta, M. L. Martínez and A. González, *Foods*, 2023, **12**, 3833.

26 S. Amariei, F. Ursachi and A. Petraru, *Membranes*, 2022, **12**, 576.

27 T. Jurić, D. Uka, B. B. Holló, B. Jović, B. Kordić and B. M. Popović, *J. Mol. Liq.*, 2021, **343**, 116968.

28 I. Toledo-Manuel, M. Pérez-Alvarez, G. Cadenas-Pliego, C. J. Cabello-Alvarado, A. S. Ledezma-Pérez, J. M. Mata-Padilla, M. Andrade-Guel and C. N. Alvarado-Canché, *Ceram. Int.*, 2024, **50**, 42195–42206.

29 Z. Xia, A. Singh, W. Kiratitanavit, R. Mosurkal, J. Kumar and R. Nagarajan, *Thermochim. Acta*, 2015, **605**, 77–85.

30 N. Bensalah, K. Chair and A. Bedoui, *Sustainable Environ. Res.*, 2018, **28**, 1–11.

31 S. Krukowski, M. Karasiewicz and W. Kolodziejski, *J. Food Drug Anal.*, 2017, **25**, 717–722.

32 B. Liu, H. Ye, Q. Liang, L. Jiang, M. Chen and S. Yang, *J. Sci. Food Agric.*, 2023, **103**, 1964–1973.

33 X. Zhang, X. Chen, J. Dai, H. Cui and L. Lin, *Food Hydrocolloids*, 2024, **147**, 109324.

34 E. Çavdaroğlu, D. Büyüktas, S. Farris and A. Yemenicioğlu, *Food Hydrocolloids*, 2023, **135**, 108136.

35 H. Wan, Z. Zhu and D.-W. Sun, *Food Chem.*, 2024, **439**, 138114.

36 K. G. Lawal, A. Nazir, B. Sundarakani, C. Stathopoulos and S. Maqsood, *Int. J. Biol. Macromol.*, 2024, **280**, 135593.

37 T. Frangopoulos, A. Marinopoulou, A. Goulas, E. Likotrafiti, J. Rhoades, D. Petridis, E. Kannidou, A. Stamelos, M. Theodoridou, A. Arampatzidou, A. Tosounidou, L. Tsekmes, K. Tsichlakis, G. Gkikas, E. Tourasanidis and V. Karageorgiou, *Foods*, 2023, **12**, 2812.

38 J. M. Silva, C. Vilela, A. V. Girão, P. C. Branco, J. Martins, M. G. Freire, A. J. D. Silvestre and C. S. R. Freire, *Carbohydr. Polym.*, 2024, **337**, 122112.

39 P. G. Gan, S. T. Sam, M. F. Abdullah, M. F. Omar and W. K. Tan, *Polym. Degrad. Stab.*, 2021, **188**, 109563.

40 A. González, M. C. Strumia and C. I. Alvarez Igarzabal, *J. Food Eng.*, 2011, **106**, 331–338.

41 J. F. Martucci and R. A. Ruseckaite, *Polym. Degrad. Stab.*, 2009, **94**, 1307–1313.

42 H. Chen, K. Shang, X. Bian, Z. Zhao, Y. Liu, X. Lin, L. Wang, W. Zhang, X. Hu and X. Guo, *Food Packag. Shelf Life*, 2024, **46**, 101361.

43 W. Zhang, S. Roy, P. Ezati, D.-P. Yang and J.-W. Rhim, *Trends Food Sci. Technol.*, 2023, **136**, 11–23.

44 J. He, S. Yang, G. Goksen, X. Cong, M. Rizwan Khan and W. Zhang, *Food Biosci.*, 2024, **58**, 103635.

45 I. Benkhira, F. Zermane, B. Cheknane, D. Trache, N. Brosse, A. Paolone, H. Chader and W. Sobhi, *Int. J. Biol. Macromol.*, 2024, **277**, 134158.

46 J. Yang, W. Cai, M. Rizwan Khan, N. Ahmad, Z. Zhang, L. Meng and W. Zhang, *Foods*, 2023, **12**, 3336.

47 Y. Liu, J. Chen, H. Li and Y. Wang, *Int. J. Biol. Macromol.*, 2024, **259**, 128934.

48 T. I. S. Oliveira, M. F. Rosa, M. J. Ridout, K. Cross, E. S. Brito, L. M. A. Silva, S. E. Mazzetto, K. W. Waldron and H. M. C. Azeredo, *Int. J. Biol. Macromol.*, 2017, **101**, 1–8.

49 H. M. C. Azeredo, R. Morrugares-Carmona, N. Wellner, K. Cross, B. Bajka and K. W. Waldron, *Food Chem.*, 2016, **198**, 101–106.

50 H. Jiang, W. Zhang, J. Cao and W. Jiang, *Food Hydrocolloids*, 2022, **133**, 107982.

51 M. L. Fishman, D. R. Coffin, J. J. Unruh and T. Ly, *J. Macromol. Sci., Part A: Pure Appl. Chem.*, 1996, **33**, 639–654.

52 M. Fishman, D. Coffin, R. Konstance and C. Onwulata, *Carbohydr. Polym.*, 2000, **41**, 317–325.

53 Z. Fu, S. Guo, Y. Sun, H. Wu, Z. Huang and M. Wu, *Starch/Stärke*, 2021, **73**, 2000203.

54 A.-S. Hager, K. J. R. Vallons and E. K. Arendt, *J. Agric. Food Chem.*, 2012, **60**, 6157–6163.

55 M. Luangtana-anan, S. Soradech, S. Saengsod, J. Nunthanid and S. Limmatvapirat, *J. Food Sci.*, 2017, **82**, 2915–2925.

56 J. Jovanović, J. Ćirković, A. Radojković, D. Mutavdžić, G. Tanasijević, K. Joksimović, G. Bakić, G. Branković and Z. Branković, *Prog. Org. Coat.*, 2021, **158**, 106349.

57 W.-X. Du, C. W. Olsen, R. J. Avena-Bustillos, M. Friedman and T. H. McHugh, *J. Food Sci.*, 2011, **76**, M149–M155.

58 Z. Wu, J. Wu, T. Peng, Y. Li, D. Lin, B. Xing, C. Li, Y. Yang, L. Yang, L. Zhang, R. Ma, W. Wu, X. Lv, J. Dai and G. Han, *Polymers*, 2017, **9**, 102.

59 S. Belhaoues, S. Amri and M. Bensouilah, *S. Afr. J. Bot.*, 2020, **131**, 200–205.

60 P. Thunyakipisal, T. Saladyanant, N. Hongprasong, S. Pongsamart and W. Apinhasmit, *J. Investig. Clin. Dent.*, 2010, **1**, 120–125.

61 K. S. Linn, P. Kasemsiri, K. Jetsrisuparb, W. Iamamornphan, P. Chindaprasirt and J. T. N. Knijnenburg, *J. Polym. Environ.*, 2022, **30**, 2087–2098.

62 H. Kim, P. K. Panda, K. Sadeghi and J. Seo, *Prog. Org. Coat.*, 2023, **174**, 107305.

63 J. Liu, Y. Dong, X. Zheng, Y. Pei and K. Tang, *Food Chem.*, 2024, **438**, 138009.

64 Food and Agriculture Organization of the United Nations, Codex Alimentarius: Fats, Oils and Related Products. Section 1: Codex General Standard for Fats and Oils, <https://www.fao.org/4/y2774e/y2774e03.htm#TopOfPage>.

